Self-Supervised Iterative Refinement for Anomaly Detection in Industrial Quality Control

Muhammad Aqeel $^{1,2[0009-0000-5095-605X]}$, Shakiba Sharifi 1 , Marco Cristani $^1[0000-0002-0523-6042]$, and Francesco Setti $^1[0000-0002-0015-5534]$

¹ Dept. of Engineering for Innovation Medicine, University of Verona Strada le Grazie 15, Verona, Italy ² muhammad.ageel@univr.it

Abstract. This study introduces the Iterative Refinement Process (IRP), a robust anomaly detection methodology tailored for high-stakes industrial quality control. The IRP systematically enhances defect detection accuracy by employing a cyclic data refinement strategy that iteratively removes misleading data points, thereby improving the model's performance and robustness. We validate the effectiveness of the IRP using two benchmark datasets, Kolektor SDD2 (KSDD2) and MVTec-AD, covering a wide range of industrial products and defect types. Our experimental results demonstrate that the IRP consistently outperforms traditional anomaly detection models, particularly in environments with high noise levels. This study highlights the IRP's potential to significantly enhance anomaly detection processes in industrial settings, effectively managing the challenges of sparse and noisy data.

Keywords: Robust Anomaly Detection \cdot Self Supervised Learning \cdot Iterative Refinement Process.

1 Introduction

Anomaly Detection (AD) plays an indispensable role in quality control across a wide range of manufacturing industries, ensuring the integrity of materials such as marble [1], steel [2], and leather [3]. Accurately detecting items that are non-compliant with product specifications is crucial for maintaining product standards and consumer satisfaction. However, this task is fraught with challenges, primarily due to the diverse and complex textures of the materials, the rarity of defects, and the significant scarcity of accurately labeled data necessary for effective supervised learning. Anomalies typically occupy only a tiny portion of an image, making their detection difficult for human inspectors and automated systems. This challenge is compounded by the labor-intensive and error-prone nature of manually labeled training data, a process that becomes increasingly unsustainable in high-throughput manufacturing settings.

The evolution of anomaly detection in recent years has increasingly leaned towards unsupervised learning paradigms, prized for their ability to operate without extensively labeled datasets. These approaches, while innovative, presuppose

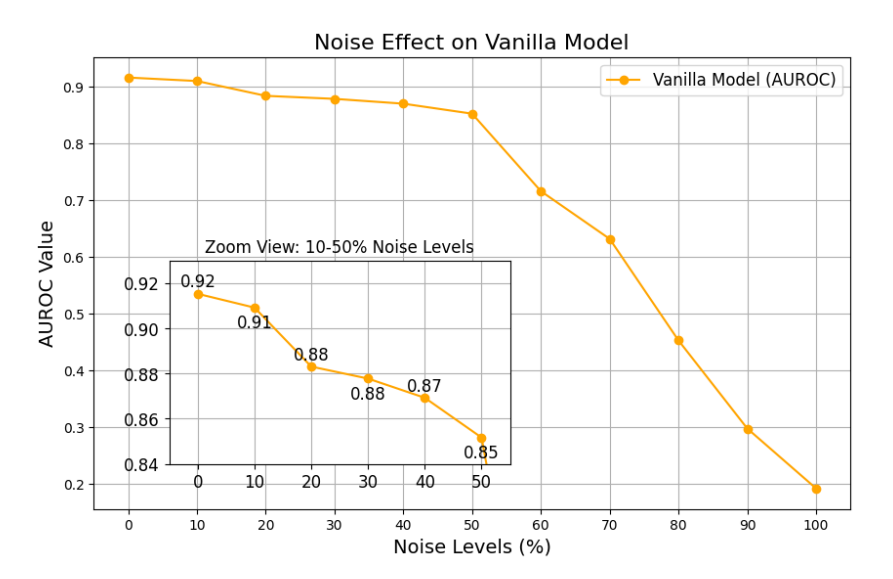


Fig. 1: Typical impact of noisy data in training an anomaly detection model.

the existence of pristine training data, free from anomalies [4,5]. This ideal is seldom met in practical scenarios, where the inclusion of even a few anomalous samples can severely skew the learning process, leading to either too restrictive or overly permissive models. Models trained under these conditions are prone to overfitting, resulting in many false positives during operational deployment. Conversely, including anomalies in the training set can escalate the incidence of false negatives, severely undermining the system's reliability.

To illustrate the severity of this issue, Fig. 1 demonstrates a decline in AU-CROC scores as noise increases in the training data. Traditional detection methods show a marked deterioration in performance as data imperfections escalate, highlighting their vulnerability. In contrast, our proposed Iterative Refinement Process (IRP) maintains a higher level of performance, showcasing its robustness and adaptability across a broad range of challenging conditions. We deliberately limit our evaluation to scenarios where the noise does not render the data overly corrupt, ensuring meaningful learning and generalization. This decision reflects our commitment to developing a method that optimally balances performance with practical applicability in realistically noisy environments.

Addressing these complexities requires a robust detection system capable of navigating the intricacies of noisy and incomplete data sets. Current advancements in deep learning, such as autoencoders [6], generative adversarial networks (GANs) [7], and discrete feature space representations [8], offer promising ways for enhancing anomaly detection. However, these technologies still struggle with determining the optimal anomaly score function, ensuring sufficient robustness against noise and outliers, and generalizing effectively to novel, unseen data sets.

In response to these ongoing challenges, this paper introduces a methodology named *Iterative Refinement Process (IRP)* specifically designed for robust anomaly detection. This process combines advanced machine learning techniques with a cyclic data refinement strategy to iteratively enhance the training dataset's quality, thereby significantly improving the model's performance and robustness. IRP systematically identifies and removes the most misleading data points based on a dynamically adjusted scoring mechanism, thereby refining the model's ability to generalize from normal operational data while minimizing the influence of outliers.

The main contributions of this paper are as follows:

- We propose the Iterative Refinement Process (IRP), a robust training methodology that employs a cyclic refinement strategy to enhance data quality and model accuracy in anomaly detection systematically;
- The dynamic threshold adjustment mechanism adapts the exclusion threshold based on a robust statistical measure, ensuring precise and adaptive outlier removal. This feature enhances the system's ability to accurately identify and exclude data points that do not conform to the expected pattern, improving overall detection performance.
- We present an experimental validation of our proposed methodology across two challenging public datasets, namely KSDD2 and MVTec-AD, demonstrating significant improvements over traditional approaches and establishing a new standard for robustness in the field.

2 Related Work

Detecting and identifying defects is crucial in manufacturing to ensure processes function correctly. Anomaly detection involves identifying issues such as scratches, blemishes, blockages, discoloration, holes, and, in general, any surface or structural irregularity on a manufactured item [9]. Recent surveys review AD's state of the art from both technological and methodological perspectives [10,11]. Traditionally, AD can be formulated as a supervised or unsupervised learning problem. Supervised methods use both anomaly and normal samples during training, while unsupervised methods only use normal samples at training time. While supervised methods achieve better results, the high cost of annotated datasets and advances in generative AI have shifted focus towards unsupervised approaches. Many unsupervised methods rely on image reconstruction using encoder-decoder networks to spot anomalies by comparing original and reconstructed images [12,13,14]. These networks struggle to reconstruct anomalous regions accurately, having never encountered them during training, which can result in high false positive rates with variable training data. To address this, [15] employs a reconstruction network to restore normal appearances in anomalous images, while another approach introduces textual prompts describing defects as in [16,17]. Comparing features instead of whole images also helps to reduce false positives [6,18].

4 M. Ageel et al.

Robust anomaly detection (RAD) addresses the problem of mitigating the effect of bad annotations in the training set. It has been widely studied in several fields, using methods ranging from robust statistical techniques [19] to deep learning approaches like autoencoders [5,20] and recurrent neural networks [21]. These methods all aim to reduce sensitivity to noise in the labeling process. Alternatively, [22] focused on removing noisy labels while using high-performing anomaly detectors. Here, a two-layer online learning framework filters suspicious data and detects anomalies from the remaining data. We argue that training two different models (one for predicting data quality and one for anomaly detection) adds unnecessary complexity. More recently, researchers have explored self-supervised learning (SSL). Most of the works rely on adaptations of deep CNN for enhancing learning capabilities from unlabelled data [23,24,25], or using domain-adaptation techniques [26]. In our previous work [27], we showed that SSL could also be effective in filtering badly labeled data in the training set. In this paper, we extend the previous work by using an iterative approach that is based on statistical observations of anomaly score estimation on the training set.

3 Iterative Refinement Process

The Iterative Refinement Process (IRP) introduces a novel approach to significantly enhance the robustness and accuracy of anomaly detection in an industrial environment by applying advanced probabilistic models to iteratively refine the training dataset. Despite being agnostic with respect to the anomaly detection model, for our preliminary evaluation of the impact of our approach, we used the DifferNet model [18], which provided foundational insights into the potential refinements necessary for handling complex anomaly detection in industrial settings. The DifferNet model employs a normalizing flow-based architecture to provide precise density estimations of image features extracted via a convolutional neural network. DifferNet establishes a bijective relationship between the feature space and the latent space, enabling each vector to be uniquely mapped to a likelihood score. This scoring is derived from the model's ability to discern common patterns from uncommon ones, making it especially effective for detecting subtle anomalies often found in defect detection scenarios. Initially, each data point, x_i , is evaluated using a probabilistic model tailored to anomaly detection, calculating an anomaly likelihood as follows:

$$A(x_i) = -\log p(x_i; \theta) \tag{1}$$

where $p(x_i; \theta)$ is the probability density function of data points with the model parametrization of θ . The framework engages in a dynamic data refinement cycle, where each point is assessed against an adaptive threshold calculated as T times the median of the anomaly scores, $A(x_i)$. If any data point's anomaly score exceeds this threshold, it is removed to refine the dataset. The refined dataset, denoted D_{new} , excludes the most anomalous data point, x_{max} , where x_{max} is the point with the maximum anomaly score exceeding the threshold. This

Algorithm 1 Iterative Refinement and Retraining

```
1: Input: Dataset of images D = \{x_1, x_2, \dots, x_n\}
 2: Pre-train model on D for N epochs
 3: Compute anomaly scores A = \{a_1, a_2, \dots, a_n\} where a_i = -\log p(x_i; \theta)
 4: Compute median of scores M = \text{median}(A) \triangleright \text{Median score used for thresholding}
 5: if \max(A) > T \times M then
 6:
        x_{\text{max}} \leftarrow x_i \text{ where } a_i = \max(A)
 7:
        Delete x_{\text{max}} from D
         D_{\text{new}} \leftarrow D \setminus \{x_{\text{max}}\}
 8:
9: else
         D_{\text{new}} \leftarrow D
10:
11: end if
12: Retrain model on D_{\text{new}}
13: repeat
14:
         Repeat steps 3 to 9 until the specified number of epochs is reached
15: until Maximum epochs reached
```

process of refinement and retraining on D_{new} continues until the dataset achieves optimal stability and performance. The steps involved in this refinement process are elaborated in Algorithm 1, and the entire sequence from data input through anomaly detection, refinement, and final evaluation is illustrated in Fig. 2.

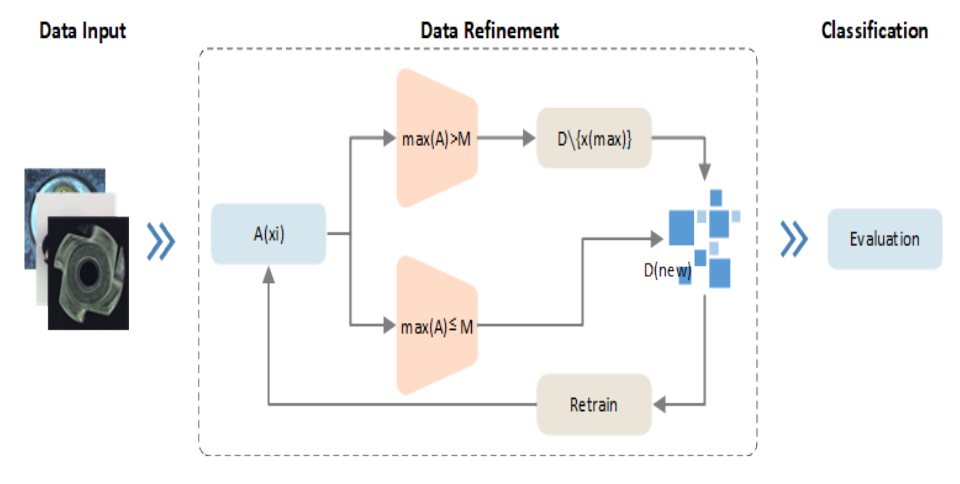


Fig. 2: Illustrative schematic of the Iterative Refinement Process, demonstrating the independent cycle of training, validation, retraining, and testing.

3.1 Probabilistic Anomaly Scoring Mechanism and Dynamic Refinement

Integral to DifferNet's approach is a robust probabilistic scoring system that enhances the accuracy and robustness of defect detection through dynamic refinement processes. This anomaly detection framework utilizes a convolutional neural network (CNN) as a pretrained feature extractor, denoted as f_{ex} , which is not optimized further post-training. This extractor transforms input data $x \in X$ into a feature space Y, specifically:

$$y = f_{ex}(x) \in Y \tag{2}$$

These extracted features y are further processed by a state-of-the-art normalizing flow model f_{NF} , which maps them into a well-defined latent space Z with a known distribution $p_Z(z)$. This transformation is crucial as it enables the precise estimation of the data's likelihood based on the latent representation:

$$z = f_{NF}(y)$$
 where $z \sim \mathcal{N}(0, I)$ (3)

Anomaly scores are computed directly from the latent space using the likelihood of the transformed features. Lower likelihood values indicate higher probabilities of an anomaly due to the deviation of features from the model of 'normal' data. These scores are calculated by averaging the negative log-likelihoods of multiple transformed instances of an image x, which are obtained using a set of predefined transformations T:

$$\tau(x) = \mathbb{E}_{T_i \in T}[-\log p_Z(f_{NF}(f_{ex}(T_i(x))))] \tag{4}$$

Our significant contribution is manifest in the dynamic adjustment of the assessment threshold θ , which is iteratively recalibrated in response to evolving data characteristics and directly influenced by the statistical nature of the anomaly scores:

Threshold =
$$T \times M$$
 (5)

Data points whose anomaly scores exceed this threshold are considered outliers and are subsequently removed from the dataset:

$$D_{\text{new}} = D_{\text{old}} \setminus \{x \mid \tau(x) > \text{Threshold}\}$$
 (6)

This iterative refinement process not only enhances the quality and performance of the model but also stabilizes it at an optimal level. Moreover, this method is designed not only to detect but also localize anomalies within images, leveraging the gradient of the loss function to clearly demarcate regions contributing to anomalies, thus providing a robust mechanism for practical deployment in industrial quality control systems.

4 Experimental Results

This section presents the experimental results obtained from applying the Iterative Refinement Process (IRP) to anomaly detection. The experiments were designed to evaluate the effectiveness of the IRP in improving detection accuracy and robustness under various conditions.

4.1 Datasets

We assess the performance of our approach using two publicly available datasets, which are extensively used to assess the robustness and effectiveness of defect detection models:

Kolektor SDD2 (KSDD2): The KSDD2 dataset [2] consists of RGB images showcasing defective production items, meticulously sourced and annotated by Kolektor Group d.o.o. The defects vary widely in size, shape, and color, ranging from minor scratches and spots to significant surface faults. For uniform evaluation, all images are center-cropped and resized to dimensions of 448 x 448 pixels. The training set comprises 2085 normal samples and 246 positive samples, while the testing set includes 894 negative samples and 110 positive samples.

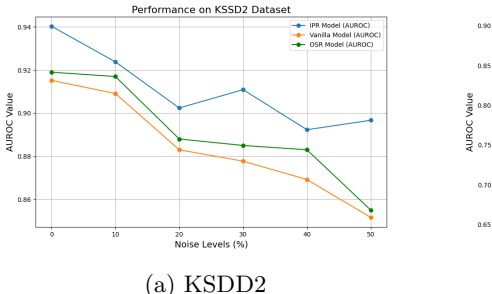
MVTec-AD Dataset: The MVTec-AD dataset [28] is utilized to demonstrate the effectiveness of our proposed method across a variety of real-world industrial products. The MVTec-AD dataset contains 15 different types of industrial products, encompassing over 70 different types of defects, each labelled with both defect types and segmentation masks. To address the original lack of defective images in the training set, we resampled half of the defect images to include in our training data. The revised training set contains 889 normal and 1345 defective images, while the testing set comprises 1210 normal and 724 defective images.

4.2 Implementation Details

Experiments were conducted using PyTorch on NVIDIA GPUs, specifically utilizing CUDA. Our model processes images resized to 448 × 448 pixels, with standardized preprocessing that includes optional rotations and normalization using means of [0.485, 0.456, 0.406] and standard deviations of [0.229, 0.224, 0.225]. The network architecture features three scales of input resolution, 8 coupling blocks within the normalizing flow model, and fully connected layers in the scale-translation networks each containing 2048 neurons, with no dropout our proposed method's effectiveness across various applied. Training parameters are set with a learning rate of 2×10^{-4} , and the model undergoes 400 epochs with batch size 96. Data augmentation involves multiple transformations per sample, with 4 in training and 64 in testing to ensure robustness. Outputs are managed with verbose logging for detailed monitoring, optional gradient map visualization, and periodic model saving to capture progress and facilitate ongoing optimization.

4.3 Varying Noise Levels on KSDD2

In this study, we rigorously evaluate the robustness and efficacy of the Iterative Refinement Process (IRP) on the KSDD2 dataset. Our analysis delves into the performance dynamics of the IRP model under various noise conditions, revealing its exceptional defect detection capabilities in the face of escalating environmental challenges. As illustrated in Fig. 3, the IRP model is compared



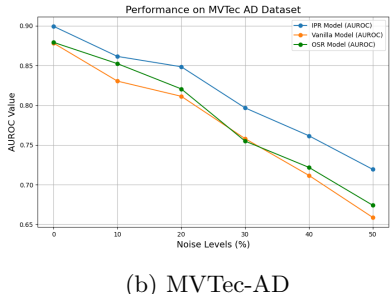


Fig. 3: Figure (a) displays the performance trends of various models on the KSDD2 dataset, while figure (b) shows results for the MVTec-AD dataset, across different noise levels. The graphs illustrate the models' performance before and after applying the IPR model: the blue line represents the IPR model, the green line denotes the OSR model, and the yellow line illustrates the performance of the vanilla model.

against two conventional approaches—the traditional vanilla model and the One Shot Removal (OSR) model proposed in [27]. Across all tested noise levels, the IRP model consistently outperforms the competitors, demonstrating remarkable resilience by maintaining superior AUROC values, as systematically documented in Table 1.

The IRP model's prowess is particularly pronounced at elevated noise levels. For instance, at a substantial noise threshold of 50%, the IRP model sustains a significantly higher AUROC of 0.8967 on the KSDD2 dataset. This performance starkly contrasts with the pronounced declines observed in the vanilla and OSR models. This robustness is not merely a result of the algorithm's inherent strength but arises from the IRP's comprehensive application of advanced noise-cancellation algorithms, adaptive thresholding techniques, and its capacity to effectively extract complex features from heavily corrupted data streams.

Moreover, the statistical analysis accompanying our findings reinforces the IRP model's superiority. The standard deviation values reported in Table 1 indicate lower variability in performance across different experimental runs, underscoring the model's reliability and predictability. Such attributes are indispensable in industrial applications, where the cost of false negatives can be prohibitive, and the ability to detect anomalies reliably is paramount. The comprehensive data presented in the table not only showcases the IRP model's adaptability and robust performance across diverse and challenging scenarios but also highlights its viability as a potent tool for maintaining stringent quality control standards in manufacturing processes. These findings suggest that the IRP can be effectively deployed in industrial settings to enhance defect detection where traditional models might falter due to high variability in defect rates and challenging noise conditions.

4.4 Varying Noise Levels on MVTec-AD

The robustness and adaptability of IRP have been rigorously evaluated across various product classes within the MVTec-AD dataset, including Cable, Capsule, MetalNut, Pill, Screw, and Zipper. Each class, with its distinct defect types and unique challenges, served as an ideal testbed for the IRP. We systematically varied the noise levels in the dataset from 0% to 50% to meticulously assess the IRP's capabilities under progressively challenging conditions, using the Area Under the Curve of the Receiver Operating Characteristic (AUROC) to quantify defect detection accuracy across different thresholds.

As illustrated in Fig. 4, the IRP model consistently achieves high AUROC values across all classes, demonstrating its robust ability to manage noise effectively. Notably, in classes with complex and variable defect characteristics such as Screw and Cable, the IRP exhibits exceptional resilience, showcasing its advanced anomaly detection capabilities. Conversely, in classes like Capsule and Pill, where defects are more subtle, the IRP effectively distinguished between normal variations and actual defects, underlining its sophisticated feature extraction capabilities. This uniform performance across varied classes and noise levels highlights the IRP model's versatility and effectiveness in industrial applications, especially in settings where defect rates are unpredictable and varied. The IRP's ability to maintain high accuracy at elevated noise levels underscores its potential as a dependable tool for quality control in manufacturing environments.

Furthermore, Fig. 3 provides an overarching view of the IRP's performance across the MVTec-AD dataset. This visual representation emphasizes the IRP's superior performance relative to the vanilla and OSR models, particularly as it consistently improves defect handling under increasingly challenging conditions. This enhancement affirms the IRP's role as a robust and reliable quality control instrument in complex manufacturing landscapes, where defect rates can fluctuate significantly. Table 1 complements these insights by detailing the AUROC scores at various noise levels for both the MVTec-AD and KSDD2 datasets, including measures of error magnitude. This detailed presentation not only confirms the performance stability of the IRP across different settings but also highlights the model's reliability, evidenced by the low standard deviation in its performance metrics.

Table 1: AUROC scores of the IRP model at different noise levels for MVTec-AD and KSDD2 datasets.

Noise Level	(%) Capsule	Cable	${\bf Metal Nut}$	Pill	Screw	\mathbf{Zipper}	MVTec-AD	KSDD2	Error Magnitude
0%	0.8592	0.9288	0.8880	0.8888	0.8938	0.9378	0.8994	0.9403	± 0.0246
10%	0.8498	0.8368	0.8688	0.8580	0.868	0.8880	0.8615	0.9238	± 0.0149
20%	0.8288	0.856	0.8480	0.8558	0.8524	0.8504	0.8485	0.9024	± 0.0086
30%	0.8102	0.6756	0.8464	0.8016	0.8234	0.8232	0.7967	0.9109	± 0.0518
40%	0.8012	0.5716	0.7792	0.8096	0.7988	0.8096	0.7616	0.8923	± 0.0777
50%	0.7872	0.4604	0.8096	0.7816	0.7436	0.7340	0.7193	0.8967	± 0.1099

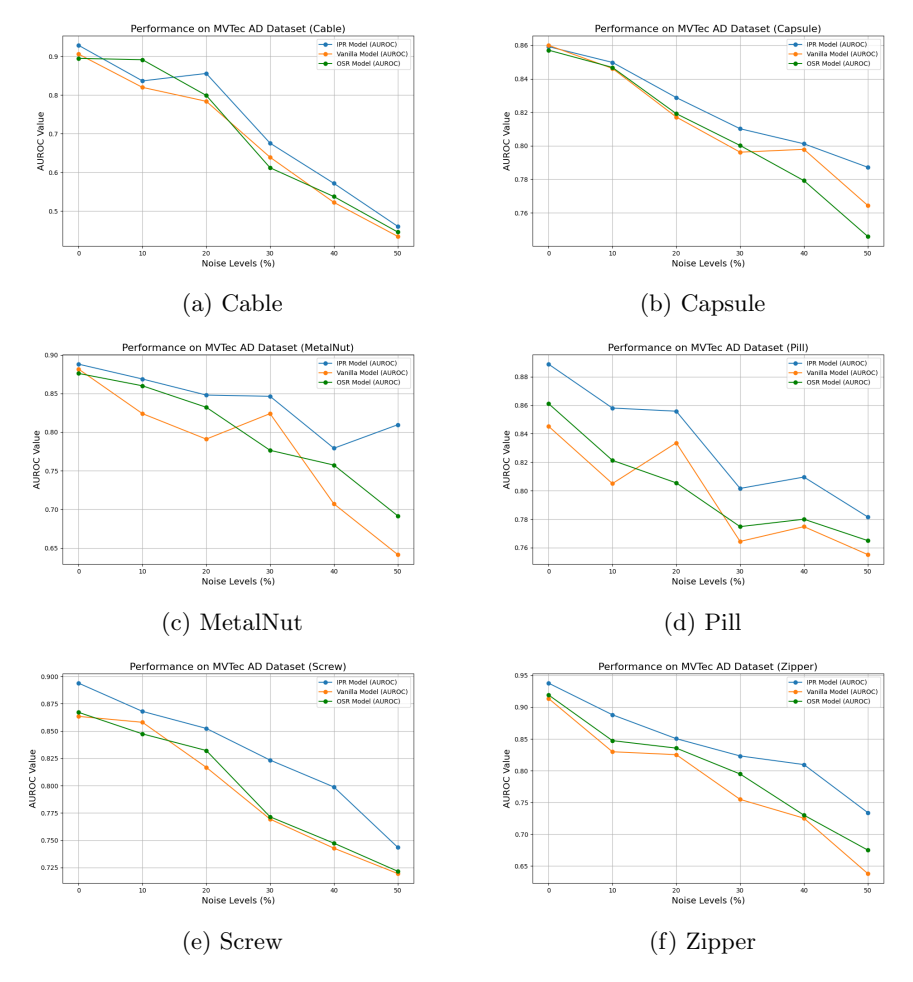


Fig. 4: AUROC performance of the IRP across various classes of the MVTec-AD dataset. Each sub-figure demonstrates the defect detection efficacy for a different class, illustrating the robustness and adaptability of the IRP in handling diverse defect characteristics.

4.5 Quantitative Analysis of Removed Samples

In this section, we present a detailed quantitative analysis of the samples removed during the defect detection process for both the KSDD2 and MVTec-AD datasets. This analysis is segmented by product categories and noise levels, providing insights into the effectiveness of the Iterative Refinement Process (IRP) in improving defect detection accuracy. Table 2 shows the number of good and bad samples removed at various noise levels (0% to 50%) across different product categories within the KSDD2 and MVTec-AD datasets. The categories include

Cable, Capsule, Metalnut, Pill, Screw, and Zipper. Each entry in the table specifies the count of good (non-defective) and bad (defective) samples removed during the training and validation phases. The accompanying graph Fig. 5 provides a visual representation of the number of good and bad samples removed at each noise level, helping to understand the distribution and trends of sample removal across different noise conditions.

Table 2: Images deleted at various noise levels for KSDD2 and MVTec-AD datasets, segmented by product categories.

	KSE	DD_2	\mathbf{MvTec}												
Noise Level (%)			Cable		Capsule		Metalnut		Pill		Screw		Zipper		
	$\overline{\text{Good}}$	Bad	$\overline{\text{Good}}$	Bad	Good	Bad	$\overline{\text{Good}}$	Bad	$\overline{\text{Good}}$	Bad	$\overline{\text{Good}}$	Bad	Good	Bad	
0%	11	0	6	0	16	0	14	0	17	0	15	0	19	0	
10%	3	5	5	7	11	6	6	8	9	8	12	5	10	5	
20%	3	7	5	9	5	12	5	11	5	11	6	9	8	9	
30%	2	8	4	11	4	14	3	11	4	13	7	11	5	11	
40%	4	12	3	12	2	13	2	9	5	12	6	10	6	14	
50%	4	13	4	12	5	13	1	9	3	11	2	12	5	13	

The table indicates that at 0% noise, only good samples are removed. This might seem counterintuitive, but it can be explained by the fact that these good samples are likely close to the decision boundary, making them appear anomalous during the initial iterations of the IRP. Removing these borderline good samples helps in refining the model by reducing potential noise and improving its generalization capability. This phenomenon demonstrates the IRP's ability to fine-tune the model even when no actual bad samples are present. As noise levels increase, the number of bad samples removed rises, which is expected. However, the table also shows that good samples continue to be removed across all noise levels. This ongoing removal of good samples close to the boundary helps in maintaining the robustness of the model by continuously refining its decision boundaries.

The quantitative analysis of removed samples underscores the IRP model's capacity to enhance defect detection accuracy through systematic refinement. By removing samples close to the decision boundary, the IRP improves the overall performance, even in the absence of bad samples. As noise levels increase, the model adeptly identifies and eliminates defective samples while maintaining a balance by also removing borderline good samples. This approach not only fine-tunes the model but also ensures its robustness and reliability in real-world industrial applications.

5 Discussion

The robust performance of the IRP across varying noise levels underscores its potential utility in industrial settings, where defect patterns may be unpredictable.

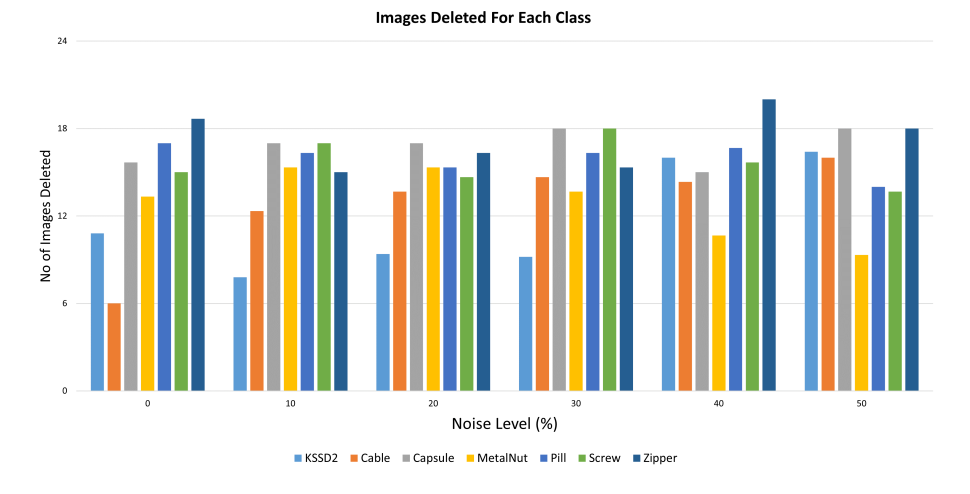


Fig. 5: This graph shows the number of good and bad samples removed at various noise levels, illustrating the distribution and trends in sample removal under different noise conditions.

The model's ability to maintain high AUROC values under increasing noise conditions illustrates its capacity to effectively distinguish subtle defect features from normal variability an essential attribute for critical quality control environments.

While the model demonstrates strong performance, there is scope to enhance its operational efficiency. The current training setup, designed for moderate scale and tailored to specific experimental conditions, serves well under controlled scenarios. However, as we aim to deploy the model in more dynamic industrial settings, optimizing its capacity to handle larger datasets and faster processing cycles will be crucial. These enhancements are intended to reduce the time required to reach model convergence and increase the throughput of image processing, ensuring the model can meet the demands of real-time defect detection. Future developments could include refining the training algorithms to accelerate convergence without compromising accuracy, and expanding the system's architecture to support more simultaneous operations. These improvements will be critical for deploying the model in environments where rapid decision-making is essential. Furthermore, the detailed analysis of different classes within the MVTec-AD dataset highlights the IRP's adaptability to diverse manufacturing scenarios. The pronounced resilience in classes with intricate defect patterns, such as Screws and Cables, underscores the model's sophisticated feature recognition capabilities, which are likely bolstered by advanced data preprocessing and anomaly scoring mechanisms. Moving forward, additional research could focus on optimizing the model to enhance detection accuracy in scenarios with extremely subtle defect signals, such as those found in high-grade pharmaceutical manufacturing.

Future research efforts might also refine the probabilistic models used within the IRP, enhancing their sensitivity to minor anomalies and incorporating real-time learning capabilities to dynamically adapt to new types of defects as they emerge. Addressing the current limitations by increasing the processing capacity of the model and reducing dependency on lengthy epoch training will be key. Additionally, exploring the integration of the IRP with other industrial monitoring systems could broaden its applicability, ensuring it remains a versatile and effective tool in the rapidly evolving landscape of manufacturing technologies.

6 Conclusions

The experimental validation of the Iterative Refinement Process (IRP) presented in this study underscores its substantial efficacy in enhancing anomaly detection across diverse industrial settings. Employing robust statistical measures and sophisticated anomaly scoring mechanisms, the IRP has consistently demonstrated superior performance over traditional methods such as the vanilla model and One Shot Removal (OSR) model, particularly in environments characterized by high noise levels. Through rigorous testing on the KSDD2 and MVTec-AD datasets, the IRP not only achieved high AUROC scores but also exhibited remarkable resilience against variable noise intensities, effectively maintaining its defect detection capabilities even under challenging conditions. The system's ability to accurately distinguish between defective and non-defective items, even with subtle defect features, highlights its potential as a critical tool for maintaining high standards in industrial quality control. These results validate the effectiveness of the IRP, showcasing its adaptability to different defect types and its robust performance across a spectrum of industrial products. The study's outcomes suggest that the IRP can greatly enhance the precision and reliability of defect detection systems, ensuring significant improvements in quality assurance processes within manufacturing environments.

Acknowledgments. This study was carried out within the PNRR research activities of the consortium iNEST (Interconnected North-Est Innovation Ecosystem) funded by the European Union Next-GenerationEU (Piano Nazionale di Ripresa e Resilienza (PNRR) – Missione 4 Componente 2, Investimento 1.5 – D.D. 1058 23/06/2022, ECS_00000043).

Disclosure of Interests. The authors declare that they have no conflict of interest.

References

- Vrochidou, E., Sidiropoulos, G.K., Ouzounis, A.G., Lampoglou, A., Tsimperidis, I., Papakostas, G.A., Sarafis, I.T., Kalpakis, V., Stamkos, A.: Towards robotic marble resin application: Crack detection on marble using deep learning. Electronics 11(20) (2022)
- 2. Božič, J., Tabernik, D., Skočaj, D.: Mixed supervision for surface-defect detection: from weakly to fully supervised learning. Computers in Industry (2021)
- 3. Jawahar, M., Anbarasi, L.J., Geetha, S.: Vision based leather defect detection: a survey. Multimedia Tools and Applications 82(1) (2023) 989–1015

- Ono, Y., Tsuji, A., Abe, J., Noguchi, H., Abe, J.: Robust detection of surface anomaly using lidar point cloud with intensity. The International Archives of the Photogrammetry, Remote Sensing and Spatial Information Sciences 43 (2020) 1129–1136
- Beggel, L., Pfeiffer, M., Bischl, B.: Robust anomaly detection in images using adversarial autoencoders. In: European Conference on Machine Learning and Knowledge Discovery in Databases (ECML-PKDD). (2020)
- Zavrtanik, V., Kristan, M., Skočaj, D.: DSR-a dual subspace re-projection network for surface anomaly detection. In: European Conference on Computer Vision (ECCV). (2022)
- 7. Luo, Z., He, K., Yu, Z.: A robust unsupervised anomaly detection framework. Applied Intelligence **52**(6) (2022) 6022–6036
- 8. Hu, M., Wang, Y., Feng, X., Zhou, S., Wu, Z., Qin, Y.: Robust anomaly detection for time-series data (2022)
- De Vitis, G.A., Foglia, P., Prete, C.A.: Row-level algorithm to improve real-time performance of glass tube defect detection in the production phase. IET Image Processing 14(12) (2020) 2911–2921
- Chen, Y., Ding, Y., Zhao, F., Zhang, E., Wu, Z., Shao, L.: Surface defect detection methods for industrial products: A review. Applied Sciences 11(16) (2021) 7657
- Bhatt, P.M., Malhan, R.K., Rajendran, P., Shah, B.C., Thakar, S., Yoon, Y.J., Gupta, S.K.: Image-based surface defect detection using deep learning: A review. Journal of Computing and Information Science in Engineering 21(4) (2021) 040801
- Akcay, S., Atapour-Abarghouei, A., Breckon, T.P.: GANomaly: Semi-supervised anomaly detection via adversarial training. In: Asian Conference on Computer Vision (ACCV). (2019)
- Defard, T., Setkov, A., Loesch, A., Audigier, R.: Padim: a patch distribution modeling framework for anomaly detection and localization. In: International Conference on Pattern Recognition (ICPR). (2021)
- 14. Roth, K., Pemula, L., Zepeda, J., Schölkopf, B., Brox, T., Gehler, P.: Towards total recall in industrial anomaly detection. In: IEEE/CVF Conference on Computer Vision and Pattern Recognition (CVPR). (2022)
- 15. Zavrtanik, V., Kristan, M., Skočaj, D.: Draem-a discriminatively trained reconstruction embedding for surface anomaly detection. In: IEEE/CVF International Conference on Computer Vision (ICCV). (2021)
- Capogrosso, L., Girella, F., Taioli, F., Chiara, M., Aqeel, M., Fummi, F., Setti, F., Cristani, M., et al.: Diffusion-based image generation for in-distribution data augmentation in surface defect detection. In: International Joint Conference on Computer Vision, Imaging and Computer Graphics Theory and Applications. Volume 2., SciTePress (2024) 409–416
- 17. Girella, F., Liu, Z., Fummi, F., Setti, F., Cristani, M., Capogrosso, L.: Leveraging latent diffusion models for training-free in-distribution data augmentation for surface defect detection. In: International Conference on Content-based Multimedia Indexing (CBMI). (2024)
- 18. Rudolph, M., Wandt, B., Rosenhahn, B.: Same same but different: Semi-supervised defect detection with normalizing flows. In: IEEE/CVF Winter Conference on Applications of Computer Vision. (2021)
- 19. Rousseeuw, P.J., Hubert, M.: Anomaly detection by robust statistics. Wiley Interdisciplinary Reviews: Data Mining and Knowledge Discovery 8(2) (2018) e1236
- Zhou, C., Paffenroth, R.C.: Anomaly detection with robust deep autoencoders.
 In: ACM SIGKDD International Conference on Knowledge Discovery and Data Mining. (2017)

- Su, Y., Zhao, Y., Niu, C., Liu, R., Sun, W., Pei, D.: Robust anomaly detection for multivariate time series through stochastic recurrent neural network. In: ACM SIGKDD International Conference on Knowledge Discovery and Data Mining. (2019)
- Zhao, Z., Birke, R., Han, R., Robu, B., Bouchenak, S., Mokhtar, S.B., Chen, L.Y.: Rad: On-line anomaly detection for highly unreliable data. arXiv preprint arXiv:1911.04383 (2019)
- Božič, J., Tabernik, D., Skočaj, D.: End-to-end training of a two-stage neural network for defect detection. In: International conference on pattern recognition (ICPR), IEEE (2021)
- Zhang, C., Wang, Z., Liu, B., Xiaolei, W., et al.: Steel plate defect recognition of deep neural network recognition based on space-time constraints. Advances in Multimedia 2022 (2022)
- Tian, R., Jia, M.: Dcc-centernet: A rapid detection method for steel surface defects. Measurement 187 (2022) 110211
- Zhang, S., Zhang, Q., Gu, J., Su, L., Li, K., Pecht, M.: Visual inspection of steel surface defects based on domain adaptation and adaptive convolutional neural network. Mechanical Systems and Signal Processing 153 (2021) 107541
- 27. Aqeel, M., Sharifi, S., Cristani, M., Setti, F.: Self-supervised learning for robust surface defect detection. In: International Conference on Deep Learning Theory and Applications (DELTA). (2024)
- 28. Bergmann, P., Fauser, M., Sattlegger, D., Steger, C.: Mvtec ad–a comprehensive real-world dataset for unsupervised anomaly detection. In: Proceedings of the IEEE/CVF conference on computer vision and pattern recognition. (2019) 9592–9600